27 June 1997

ELSEVIER

Chemical Physics Letters 272 (1997) 257–264

CHEMICAL PHYSICS LETTERS

An experimental investigation of the effect of rotation on the rate of unimolecular decomposition of NO_2

P.I. Ionov [1], I. Bezel, S.I. Ionov [2], C. Wittig

Department of Chemistry, University of Southern California, Los Angeles, CA 90089, USA

Received 23 December 1996; in final form 26 March 1997

Abstract

The effect of rotational excitation on the rate of unimolecular decomposition has been examined for a benchmark system. NO_2 molecules having specific excitations were selected by pumping rotational components of the $(1,0,1) \leftarrow (0,0,0)$ combination band with the output from a 0.02 cm^{-1} resolution parametric oscillator, and reaction rates were obtained by applying the picosecond-resolution pump–probe technique to these tagged species. The addition of up to 100 cm^{-1} of rotational energy ($N \leqslant 15$, $K_a = 0$), with other parameters held fixed, left the rate unaffected. Implications are discussed within the framework of statistical rate theories. © 1997 Elsevier Science B.V.

1. Introduction

There are two well-known approaches to improving selectivity in photodissociation experiments: supersonic cooling and double-resonance excitation. The first, being the easier of the two to implement, has provided a wealth of high quality data in the past. However, one of its drawbacks is that reacting molecules occupy only low rotational states. Thus, since our goal was to measure the effect of rotational excitation on the unimolecular dissociation rate, it was necessary to use the second approach. This enabled dissociation rates to be measured for a set of well defined rotational excitations — in the present case for the NO_2 molecule, whose unimolecular decomposition has been studied in detail [1].

The experimental strategy is to optically excite the molecules in two steps: the first providing rotational selectivity and the second providing the time resolution necessary to measure rates. Since only molecules that absorb both photons have enough energy to react, only the rotationally selected molecules undergo decomposition (Fig. 1a). Specifically, particular rotational components of the (1, 0, 1) and (0, 0, 0) combination band of NO_2 are excited with a narrow linewidth nanosecond laser, and this is followed by application of the picosecond-resolution pump–probe technique to these tagged species. The result is that reaction rates are measured with simultaneous time and angular momentum resolution (i.e., with an N uncertainty of ± 1).

In this communication, NO_2 decomposition rates are reported for a range of initial rotational excitations that extend up to 100 cm^{-1}. The (1, 0, 1) rotational levels span the range $1 \leqslant N \leqslant 15$ (odd N, $K_a = 0$), and with the photolysis photon energy fixed, the reaction rates were found to be the same, within

[1] Present address: Applied Materials, 3320 Scott Blvd., M.S. 1114, Santa Clara, CA 95054, USA.

[2] Present address: Hughes Research Labs, 3011 Malibu Canyon Road, M.S. RL65, Malibu, CA 90265, USA.

PII S0009-2614(97)00483-1

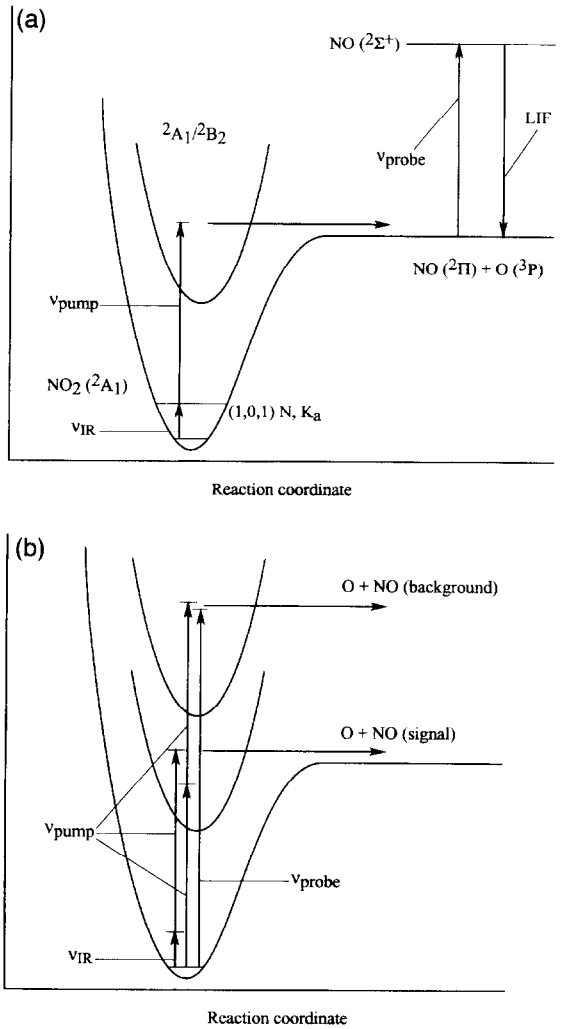

Fig. 1. (a) Double resonance approach; the high resolution IR pump provides rotational selectivity, while the subpicosecond pump and probe provides time resolution. (b) Unwanted mechanisms of producing NO.

the experimental uncertainty, for all of the N values examined.

This experiment offers a glimpse into a realm which has been largely unexplored to date. An in-depth analysis is called for, and it is not obvious a priori that simple statistical theories such as Rice, Rampsperger, Kassel and Marcus (RRKM), phase space theory (PST), and the statistical adiabatic channel (SACM) provide adequate frameworks for understanding the results. Here, the results are modeled by using RRKM theory, and good agreement with the data is obtained. Provided that this agreement is more than fortuitous, the data suggest that K_a is (at least approximately) conserved during the reaction.

2. Experimental methods

The double resonance method used in these experiments requires three pulses of radiation. The first, with wavelength near 3.4 μm and a narrow linewidth, excites a particular rotational sublevel of the (1, 0, 1) vibrational state [2]. The other two have subpicosecond durations and wavelengths of 450 and 226 nm. The former initiates NO_2 decomposition and the latter probes the NO product concentration by laser induced fluorescence (LIF). The delay between the subpicosecond pulses is scanned to obtain traces that are used later to obtain decomposition rates.

Much of the experimental arrangement has been described previously [3]. The subpicosecond pulses are obtained from a dual-jet synchronously-pumped dye laser and two dye amplifiers, with the appropriate wavelengths generated by a combination of harmonic and supercontinuum generation. Dye laser radiation (678 nm) is amplified and split in two parts. One part is tripled to give the 226 nm probe, and the other part is focused into D_2O to generate a supercontinuum. 450 nm radiation is selected from the continuum and is sent to a two-stage amplifier. The main modification to the picosecond laser system since our last report [4] is the replacement of the longitudinally pumped dye cells in the red amplifier with transversely pumped ones, two of which are prism cells. This has resulted in improved beam profile and output energy.

Double resonance excitation requires a narrow-linewidth, high-intensity IR source. We used a Nd:YAG pumped KTP parametric oscillator and amplifier, which provided 3.4 μm radiation with a linewidth of ~ 0.02 cm^{-1} and typical energy of 10 mJ, which is just sufficient to saturate the (1, 0, 1) ← (0, 0, 0) transitions.

Temporal resolution is optimized by measuring the pump–probe cross correlation simultaneously with the LIF signal. The cross correlation, which is obtained by difference frequency generation in 100 μm thick BBO, is used to deconvolute the unimolec-

ular rate from the traces of LIF signal versus pump–probe delay [3]. Since the pump–probe difference frequency is close to the pump frequency, a monochromator is required to select the cross correlation signal. Despite this, a portion of the amplified spontaneous emission still falls into the spectral range of the cross correlation signal, thus requiring great care in obtaining the signal.

A major experimental obstacle is background NO due to unwanted photo-excitations (Fig. 1b) and as a result of wall-catalyzed NO_2 decomposition. Since NO_2 absorbs at 226 nm, this leads to additional NO production and spurious signals. Also, the sequential absorption of two 450 nm photons excites NO_2 to the same electronic state as does 226 nm radiation. To further complicate matters, NO can be excited with two 450 nm photons, giving additional LIF signal. The different intensity dependences of the backgrounds leads to the existence of an optimum that maximizes the signal-to-background ratio. It proved essential to optimize this ratio with respect to the intensities. Also, it was necessary to minimize surface catalyzed NO_2 decomposition and cool the sample to $T_{rot} \sim 70$ K. NO_2 is cooled in a warm molecular beam emanating from a small-orifice nozzle at low backing pressure. To minimize NO background, O_2 carrier is flowed through a glass bubbler filled with NO_2 and submerged in a 0°C slush. Also, the path from the bubbler to the supersonic nozzle entrance is made of teflon, and the O_2/NO_2 mixture is constantly pumped out from behind the valve which opens the nozzle. This minimizes the residence time of NO_2 near the valve's metal parts, which catalyze NO_2 decomposition. The above measures, along with saturation of the IR transition, resulted in a signal to background ratio of 3–5 at the maximum of the 70 K distribution. Since some of the backgrounds are time dependent, we recorded traces with the IR alternately on and off and subtracted one from the other.

3. Results

Typical scans are presented in Fig. 2. 5–6 such scans were taken for each (1, 0, 1) rotational state (odd N, $1 \leqslant N \leqslant 15$, $K_a = 0$; unresolved spin-splitting in the IR excitation step), with each scan averaged for about 4 h (200 shots at each delay time). To obtain the rates, the scans were fitted (solid lines) by using a convolution of the experimental cross correlation and a single exponential buildup [3].

Two series of measurements were carried out. In the first, a pump linewidth of 100 cm^{-1} FWHM and an excess vibronic energy given by $E_{1,0,1}(N=0) + h\nu_{pump} - D_0 = 53$ cm^{-1} were used. Since this measurement did not display any change in the rate as N was varied, we decided to repeat the measurements with a smaller pump linewidth of 30 cm^{-1} and an excess vibronic energy of 18 cm^{-1}. It was thought that increasing the contrast between the excess vibronic energy and the range of parent rotational energies would increase the likelihood of detecting a change in the rate as N was varied. In this series, special attention was paid to ensuring that long term drift of the experimental system did not cause prob-

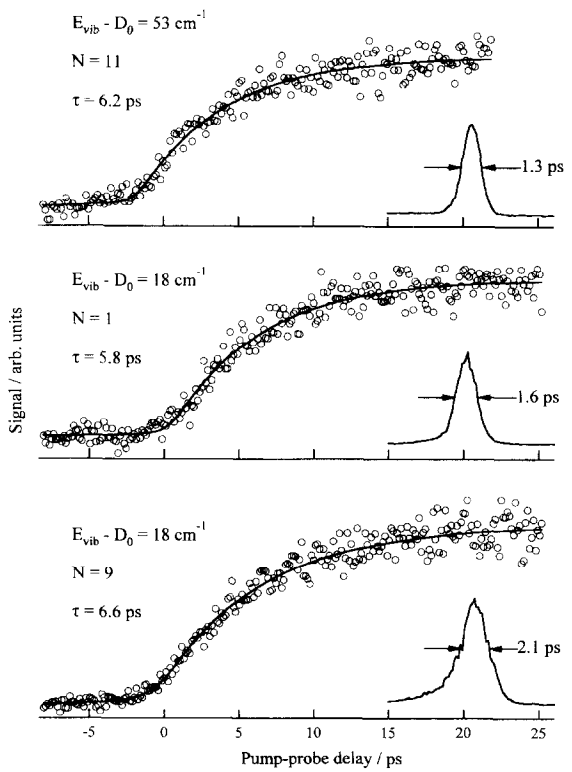

Fig. 2. Typical data showing NO LIF signal versus pump–probe delay. The corresponding cross correlation traces are to the right. The solid lines are best fits from the convolutions of single exponentials with the cross correlations.

lems. Thus, one pump–probe scan was recorded for each of the IR transitions before further scans were taken for any of the lines.

The data are summarized in Fig. 3. The rates reported here for low N are the same, within the stated uncertainties, as those measured previously [3] at the same energy by using one-photon excitation of rotationally cold NO_2. As seen in Fig. 3, there is no discernible variation of the measured rate with the (1, 0, 1) rotational level. This was not anticipated, since in the case of one-photon excitation the rate is known to be larger for a room temperature sample than for an expansion-cooled one excited with the same photon energy [3]. Taken together, these observations raise two questions which should be addressed in future experiments: (i) for $K_a = 0$, what is the maximum N value for which the rate versus N remains constant and (ii) how does the rate vary with (N, K_a)?

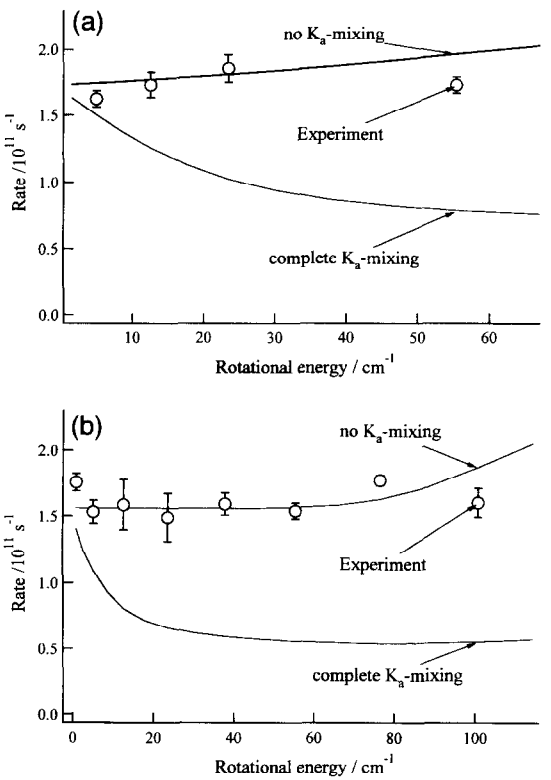

Fig. 3. Reaction rate versus rotational energy of the (1, 0, 1) intermediate level. The solid lines are RRKM calculations with complete and no K_a-mixing. In (a), the photolysis linewidth is 30 cm^{-1} FWHM, and the amount of vibronic energy in excess of D_0 is 18 cm^{-1}. In (b), these quantities are 100 cm^{-1} FWHM and 53 cm^{-1}, respectively.

4. Discussion

In this section, the experimental results are examined within the framework of simple statistical models. First, we address the question — vital for every statistical model — of how to obtain the density of levels/resonances (ρ) used in the transition state formula for the rate: $k_{tst} = W/h\rho$. Second, implications of the observed variation of the rate with rotational excitation are considered with the help of RRKM theory. Specifically, the issue of K_a-mixing is discussed.

4.1. Level densities below reaction threshold

In NO_2, most of the bright character for optical excitation is carried by the zeroth-order $^2B_2$ electronic state. This state is strongly coupled to the ground $^2A_1$ state above the conical intersection between these two surfaces, and rovibronic levels of the coupled $^2A_1/^2B_2$ system account for most of the transitions observed in the NO_2 spectrum below D_0. The density of these $^2A_1/^2B_2$ levels has been thoroughly studied by Delon et al. [5,6], and extrapolation formulas for the density of states have been derived by these authors and by Toselli and Barker [7]. These simple descriptions of the density of states work well up to a few tens of wavenumbers below D_0 (25,128.57 cm^{-1} [8]). However, just below D_0 the observed density increases markedly, diverging from the extrapolation. For example, in the 2.53 cm^{-1} region immediately below D_0, Jost et al. infer a vibronic level density of 5.4/cm^{-1} [8], which is an order of magnitude larger than the extrapolated $^2A_1/^2B_2$ value of 0.771 cm^{-1} [9]. Such a dramatic increase in the vibronic level density cannot be explained by simply invoking additional vibrational states on the coupled $^2A_1/^2B_2$ surfaces.

It is possible that the large number of observed transitions just below D_0 is due, at least in part, to the participation of additional electronic surfaces that correlate to the lowest product electronic states:

$O(^3P_2) + NO(^2\Pi_{1/2})$. In this regard, note that even potentials which are repulsive at short range may have shallow van der Waals minima at long range. For the present case of $O(^3P_J) + NO(^2\Pi_\Omega)$, the theoretical study of Graff and Wagner on the analogous $O(^3P_J) + OH(^2\Pi_\Omega)$ system serves as an excellent prototype [10]. From their work, we conclude that the surprisingly large number of transitions observed just below D_0 are probably related to the presence of shallow, long-range wells in potentials which are repulsive at short range and whose bound states are coupled to the manifold of mixed A_1/B_2 vibronic levels.

4.2. Level densities just above reaction threshold

In the following discussion, it is suggested that just above D_0 the vibronic density of $5.4/cm^{-1}$ (which was observed immediately below D_0) should be used in the transition state expression for the rate, provided that the PST number of open channels is used.

It is reasonable to assume that the high level density that exists immediately below D_0 is also present immediately above D_0, e.g., in the 5 cm^{-1} interval before the next group of open channels becomes available. Thus, it is not surprising that photoinitiated reactions using expansion-cooled NO_2 samples ($T_{rot} \cong 1$ K) result in NO yield spectra that display a high density of transitions in the 5 cm^{-1} above D_0 (i.e., approximately $14/cm^{-1}$ [11], corresponding to a vibronic density of $4.5/cm^{-1}$). This density is close to that observed just below D_0 (i.e., approximately $17/cm^{-1}$, corresponding to a vibronic density of $5.4/cm^{-1}$ [8]), also for $T_{rot} \cong 1$ K samples. Note that estimating the number of transitions that terminate on resonances above D_0 is crude because the resonances are overlapped. In many cases transitions appear as little more than phantom humplets. At higher energies the degree of overlap is larger and structure in absorption and yield spectra cannot be assigned to individual resonances.

Now consider the experimental observation of an overlapped spectrum just above D_0 — specifically, what this implies about the number of open channels and consequently the validity of PST in this energy range. For *non-overlapping* resonances, the ratio of the average separation between resonances (ρ^{-1}) to the average resonance width ($\hbar\bar{\Gamma}$) is given by

$$\frac{\rho^{-1}}{\hbar\bar{\Gamma}} = \frac{2\pi}{W}\frac{k_{tst}}{\bar{\Gamma}} = \frac{2\pi}{W}, \tag{1}$$

where use has been made of $k_{tst} = W/h\rho = \bar{\Gamma}$ for non-overlapping resonances. Thus, the region of non-overlap is characterized by $W < 2\pi$. Note that the spectrum observed in the 5 cm^{-1} above D_0 is already somewhat overlapped. In part, this overlap comes from the fact, not accounted for in Eq. (1), that transitions are obtained with $J' = 1/2$ and $3/2$. Nevertheless, one concludes from the overlap and Eq. (1) that a few channels are open. This fact, as well as the fact that the spectrum becomes even more overlapped as the energy increases over 5 cm^{-1} (which coincides with the next NO rotational state becoming energetically accessible), suggests that PST is an appropriate description for the rate in this energy regime.

Next, it is shown that there is consistency between PST and the experimental level densities and linewidths at threshold. The reaction rate is estimated by using the density of states (ρ) obtained experimentally and the numbers of open channels (W) calculated by using PST. For complete breakdown of K_a, which is known to be the case just below D_0 [8] and is assumed in PST, ρ is given by $(J_{NO_2} + 1/2)\rho_{vibr}$, where ρ_{vibr} is the density of vibronic levels ($5.4/cm^{-1}$) obtained from experiment. Note that this ρ counts only the levels of optically accessible symmetry. For $J_{NO_2} = 1/2$ and $3/2$, the numbers of open channels obtained by using PST are 4 and 8, respectively, for $NO(^2\Pi_{1/2})$ in its lowest level ($J = 1/2$). This count includes the equivalent oxygens of NO_2 and both NO Λ-doublets, but restricts open channels to those of optically accessible rovibronic symmetry. These numbers of open channels yield threshold rates of 2.2×10^{10} s^{-1} for both $J_{NO_2} = 1/2$ and $3/2$, in agreement with the values derived from linewidth analyses: 2×10^{10} s^{-1} [11] and 3×10^{10} s^{-1} [12].

As mentioned above, the high density of transitions observed just below D_0, as well as the similar density of resonances observed just above D_0, are both consistent with the participation of additional

electronic surfaces. Also, the presence of several open channels at threshold is consistent with the participation of additional electronic surfaces, since these open channels derive (at large distances) from different relative orientations of fragment electronic (including spin) angular momenta. Note that this inclusion of all available electronic surfaces is fundamental to PST, in which all combinations of angular momenta permitted by their vector addition are used to enumerate the number of open channels.

The rates reported herein for the threshold region of the pump–probe experiments (i.e., with the 30 cm^{-1} FWHM photolysis linewidth) are all approximately 1.6×10^{11} s^{-1}, which is considerably larger than the average rates obtained via lineshape analyses of the resonances in the 5 cm^{-1} above D_0 (i.e., 2×10^{10} [11] and $\sim 3 \times 10^{10}$ s^{-1} [12]). However, it should be emphasized that these different rates (i.e., those obtained via lineshape analyses versus those obtained in the present pump–probe experiments) do not constitute an inconsistency. Namely, the much larger rates obtained in the pump–probe experiments can be attributed to the larger average excess energies in these experiments. On this point, note that the broad ultrafast laser linewidths of the present experimental system make it almost impossible to probe the threshold region with high enough energy resolution to observe the rates obtained via lineshape analyses just above D_0 (e.g., the 30 cm^{-1} photolysis laser linewidth is six times larger than the entire 5 cm^{-1} interval just above D_0 over which the resonance analyses have been carried out [11,12]).

4.3. Further above reaction threshold

With increasing energy, the reaction rate increases, the transition state tightens, and weak interactions, such as those that couple the A_1 and B_2 vibronic manifolds and/or cause breakdown of the K_a quantum number, play a smaller role. This can have the effect of lessening the number of participating molecular levels. In simple terms, this is due to a competition in which a zeroth-order bright state couples both to its dissociation continuum as well as to nearby dark states, which are also coupled to dissociation continua. For the limit in which the zeroth-order bright state couples much more strongly to the continuum than to nearby dark states, the most appropriate picture is that the bright state evolves directly to the continuum without interacting with the dark states. In time-domain language, as the reaction rate increases, a regime is reached in which there is insufficient time for the optically prepared wavepacket to lose its bright state character on the time scale of the chemical reaction. For example, the loosely bound van der Waals states of the repulsive surfaces may no longer be accessed, since they are located beyond the tightened transition state. This qualitative explanation is consistent with all observations to date of photoinitiated unimolecular reactions of NO_2.

Pursuant to the above reasoning, in the calculations discussed below, the vibronic level density at the energies of the present experiments is taken as that of the coupled $^2A_1/^2B_2$ system (i.e., $0.77/cm^{-1}$, shared equally between A_1 and B_2 vibronic species). We assume that the additional level density near D_0 is related to the van der Waals wells. If this is indeed the case, such levels would be coupled to the bright states only weakly due to poor Franck–Condon factors. Thus, as the energy increases, these levels are excluded from the dissociation dynamics. The choice of $0.77/cm^{-1}$, though it fits the data well (vide infra), is ad hoc. At issue is how rapidly with increasing energy the effective level density drops from its maximum of $5.4/cm^{-1}$ at D_0 toward the density of the coupled $^2A_1/^2B_2$ system.

4.4. Effect of rotation on the reaction rate

Finally, implications of the observed variation of rate with rotational excitation are considered, specifically, the question of whether relatively weak rovibronic couplings play a role in determining the rate. RRKM theory is applied to the limiting cases of complete versus no K_a-mixing. Since the $\Delta K_a = 0$ selection rule, though not rigorous, is known to work well for strong optical transitions in NO_2 [13], it is assumed that the wavepacket prepared with the picosecond pump pulse has $K_a \cong 0$. Thus, in the case of no K_a-mixing, it is assumed that $K_a \cong 0$ throughout dissociation, i.e., in both the bound and transition state regions. Complete K_a-mixing means that all

possible K_a states have equal statistical weight. The relevant formulas are:

$$k^{\mathrm{RRKM}}_{\mathrm{mixing}}(E,N) = \frac{\sum_{-N\leq K_a\leq N} W^{\mathrm{RRKM}}_{\mathrm{V}}\left(E - E^{\ddagger}_{\mathrm{R}}(N,K_a)\right)}{h\rho_{\mathrm{VR}}(E,N)}, \quad (2)$$

$$k^{\mathrm{RRKM}}_{\mathrm{no\ mixing}}(E,N) = \frac{W^{\mathrm{RRKM}}_{\mathrm{V}}\left(E - E^{\ddagger}_{\mathrm{R}}(N,K_a=0)\right)}{h\rho_{\mathrm{V}}(E - E_{\mathrm{R}}(N,K_a=0))}, \quad (3)$$

where

$$\rho_{\mathrm{VR}}(E,N) = \sum_{-N\leq K_a\leq N} \rho_{\mathrm{V}}(E - E_{\mathrm{R}}(N,K_a)), \quad (4)$$

$$E_{\mathrm{R}}(N,K_a) = BN(N+1) + K_a^2(A-B), \quad (5)$$

$$E^{\ddagger}_{\mathrm{R}}(N,K_a) = B^{\ddagger}N(N+1) + K_a^2(A^{\ddagger} - B^{\ddagger}). \quad (6)$$

In the above, W is the number of open channels at the transition state, ρ_{V} is the vibrational density of states, E is the total energy, N is the rotational angular momentum, K_a is its internal projection, A and B are rotational constants (NO_2 is a near-symmetric top), sub-scripts V and R designate vibrational and rotational parameters, respectively, and the superscript ‡ designates the transition state.

The relevant values for the parameters used in Eqs. (2)–(6) are obtained as follows. The theoretical results of Katagiri and Kato [14] were used for the number of open channels (neglecting spin degeneracy and Λ-doublets) on the ground state surface. They obtained adiabats for the bending/hindered-rotation degree of freedom orthogonal to the reaction coordinate. These calculations give two channels open just at the threshold and a third 80 cm^{-1} above the threshold. Note that without the symmetry properties of the optically accessible states taken into account, there is a reaction path degeneracy of two due to the identical oxygens. As mentioned above, the value of $0.77/cm^{-1}$ (i.e., the density of the coupled $^2A_1/^2B_2$ system) is assigned to ρ_{V} in Eqs. (3) and (4). The rotational constants $A^{\ddagger}$ and $B^{\ddagger}$ were calculated from the assumption of a 3 Å separation between the O-atom and the NO center-of-mass and an angle of 130° for the geometry of the transition state, also taken from the work of Katagiri and Kato [14].

The distribution of reactant energies due to the picosecond pump linewidth as well as the uncertainty in the N quantum number due to the $\Delta N = \pm 1$ optical selection rule in the pico-second pump step were taken into account as follows. First, the rates were averaged over the linewidth of the picosecond laser by assuming that the measured rate is the average of the rates at specific energies. Second, the calculated rates were averaged over $N' = N'' \pm 1$, with the Hönl–London factors used as weights.

As seen in Fig. 3, the calculated rate for the case of no K_a-mixing reproduces the observed dependence of the rate on rotational energy. In contrast to this, the calculated rate for complete K_a-mixing coincides with the rate calculated for no K_a-mixing only at zero rotational energy; with increasing rotational excitation it drops markedly and is then approximately constant throughout the rest of the range examined. The physical origin of this decrease is easily understood. Since there is a large amount of rotational energy associated with the K_a quantum number (because of the large a-axis rotational constant), in the molecules with high K_a values, the available energy is insufficient to overcome the reaction threshold. Consequently, the increase in the density of states due to K_a-mixing is not compensated by an increase in the number of open channels, and therefore the rate decreases.

The good agreement between the calculated and experimental magnitudes of the rate indicates that the smaller density of $0.77/cm^{-1}$ is more consistent with the rate at the higher excess energy of the present experiments than the threshold value of $5.4/cm^{-1}$, provided RRKM theory is used. As discussed earlier, this fit can be understood as excluding the van der Waals levels from the dynamics due to the weakness of their couplings with the bright states. However, one should not overemphasize the agreement between the absolute values of the experimental and calculated rates, since neither the spacing of the open channels nor the density of $0.77/cm^{-1}$ are very reliable. Nonetheless, the conclusion that K_a is conserved is not affected by the choice of these values: the variation of the rate with N differs *qualitatively* for the limiting cases of complete and no K_a-mixing.

It is not surprising that the best fit was obtained by using no K_a-mixing, since we expect the extent

of this mixing to be small. For example, note that the 6 ps reaction time is smaller than the $NO_2(N=1, K_a=0)$ rotational period. Moreover, if $K_a=0$ is prepared initially, high K_a states are only accessible through small matrix elements and/or higher order interactions. Thus, there is a significant bias against full K_a-mixing in the present experiments.

In summary, the present results constitute an application of the double resonance method to a case in which the reaction rate is monitored in the threshold regime by recording product buildup times with picosecond resolution for differing amounts of parent rotational excitation. Such data can be used to test theoretical models. When the present results are compared to a simple application of variational RRKM theory, the picture that emerges is one of little K_a-mixing.

Acknowledgements

The authors benefited from discussions with H. Reisler, J. Troe, R. Schinke, C. Beck, S. Grebenshchikov, R.A. Beaudet and V. Mandelshtam. This research was supported by the National Science Foundation.

References

[1] S.A. Reid, H. Reisler, J. Phys. Chem. 100 (1996) 474.
[2] V. Dana, J.P. Maillard, J. Mol. Spectrosc. 71 (1978) 1.
[3] S.I. Ionov, G.A. Brucker, C. Jaques, Y. Chen, C. Wittig, J. Chem. Phys. 99 (1993) 3420.
[4] S.I. Ionov, G.A. Brucker, C. Jaques, L. Valachovic, C. Wittig, J. Chem. Phys. 99 (1993) 6553.
[5] A. Delon, R. Jost, J. Chem. Phys. 95 (1991) 5686.
[6] A. Delon, R. Jost, M. Lombardi, J. Chem. Phys. 95 (1991) 5701.
[7] B.M. Toselli, J.R. Barker, J. Chem. Phys. 91 (1989) 2239.
[8] R. Jost, J. Nygard, A. Pasinski, A. Delon, J. Chem. Phys. 105 (1996) 1287.
[9] S.I. Ionov, H.F. Davis, K. Mikhaylichenko, L. Valachovic, R.A. Beaudet, C. Wittig, J. Chem. Phys. 101 (1994) 4809.
[10] M.M. Graff, A.F. Wagner, J. Chem. Phys. 92 (1990) 2423.
[11] B. Abel, H.H. Hamann, N. Lange, J. Chem. Soc. Faraday Discuss. 102 (1997) 147.
[12] J. Miyawaki, K. Yamanouchi, S. Tsuchiya, J. Chem. Phys. 99 (1993) 254.
[13] G. Herzberg, Molecular Spectra and Molecular Structure, Krieger, Malabar, Florida, 1991.
[14] H. Katagiri, S. Kato, J. Chem. Phys. 99 (1993) 8805.